

1 **MOLECULAR CORRELATE of MOUSE EXECUTIVE FUNCTION. TOP-DOWN**
2 **and BOTTOM-UP COMPLEMENTATIONS by PRESYNAPTIC VERTEBRATE-**
3 **SPECIFIC GENE PARALOGS**

4

5 Pavel Prosselkov^{1,2*}, Qi Zhang¹, Goto Hiromichi¹, Denis Polygalov³, Thomas J. McHugh³
6 and Shigeyoshi Itohar^{1*}

7

8 ¹Laboratory for Behavioral Genetics, and ³Laboratory for Circuit and Behavior Physiology,
9 RIKEN Brain Science Institute, 351-0198 Saitama, Japan

10 ²Department of Physiology, Faculty of Medicine, Saitama Medical University, Saitama 350-
11 0495, Japan

12 *corresponding authors:

13 prosselkov@brain.riken.jp sitohara@brain.riken.jp

14

15 Keywords: executive function, attention and impulsivity, working memory, learning, gene
16 duplication, cognitive complement

17

18 **ABSTRACT**

19 Executive function (EF) is a regulatory construct of learning and a correlate of general
20 cognitive abilities. Genetic variations underlying the architecture of cognitive phenotypes are
21 likely to affect EF and associated behaviors. We have approached the behavioral variability
22 of knockout mice, as a measure of EF distortion, to calculate a proportion of a gene-specific
23 variance explained, contributing to the phenotype. Mice lacking one of *Ntng* gene paralogs,
24 encoding the vertebrate brain-specific presynaptic Netrin-G proteins, exhibit prominent
25 deficits in the EF control. Brain areas responsible for gating the bottom-up and top-down
26 information flows differentially express *Ntng1* and *Ntng2*, distinguishing neuronal circuits
27 involved in perception and cognition. As a result, high and low cognitive demand tasks
28 (HCD and LCD, respectively) modulate *Ntng1* and *Ntng2* associations either with attention
29 and impulsivity (AI) or working memory (WM), in a complementary manner. During the
30 LCD *Ntng2*-supported neuronal gating of AI and WM dominates over the *Ntng1*-associated
31 circuits. This is reversed during the HCD, when the EF requires a larger contribution of
32 cognitive control, supported by *Ntng1*, over the *Ntng2* pathways. Since human *NTNG*
33 orthologs have been reported to affect human IQ (1), and an array of neurological disorders
34 (2), we believe that mouse *Ntng* gene paralogs serve an analogous role but influencing brain
35 executive function.

36

36 INTRODUCTION

37

38 Executive function (EF) is a heterogeneous construct that can be viewed as a set of
39 processes executively supervising cognitive behaviors (3). EF is an umbrella term for
40 working memory (WM), attention and impulsivity (AI), and response inhibition, and is
41 thought to account for the variance in cognitive performance (4). WM, due to its storage and
42 processing components, is viewed as a bimodal flexible system of a limited capacity. Since
43 WM maintains current information and simultaneously supports its execution, as a latent
44 factor underlying intelligence (5), it has been termed as “the central executive” (6) attention-
45 controlling system dependent on consciousness (7). However an awareness-independent
46 model has been also proposed (8,9). General learning (Ln) ability depends on attention and
47 WM interaction (10) as well as perception, the causal and informational ground for the
48 higher cognitive functions (11). Perception guides our thinking about and acting upon the
49 world and serves as an input to cognition, via a short-term memory mediated interactions
50 (12). A possible mechanism linking perception and cognition would be attention (13).

51 Perception (bottom-up) and cognition (top-down) have been historically viewed as
52 independently operating encapsulating domains. Such embodiment has paved a ground for
53 the view that perceptual experiences can be influenced by cognitive state (for references see
54 14), consequently elaborated into the brain predictive coding approach currently dominating
55 cognitive neuroscience (15), and positing that attention is a property of brain computation
56 network (16). However this has been challenged by the opposite opinion that “Cognition
57 does not affect perception” (17). Regardless whether or not such a cognitive-sensory
58 dichotomy exists, herein we view perception and cognition as two main information streams
59 the EF exerts its actions upon, possibly through active association.

60 We have previously described the function of two vertebrate-specific brain-expressed
61 presynaptic gene paralog, *NTNG1* and *NTNG2*, complementary affecting verbal
62 comprehension and WM in human subjects, which underwent an accelerated evolution in
63 primates and extinct hominins (1). This pair of genes is also implicated in the phenomena of
64 antagonistic pleiotropy, a trade-off between the evolution-driven cognitive function
65 elaboration and an array of concomitant neuropathologies, rendering the human brain
66 phenotypically fragile (2). *Ntngs* also complementary diversify the mouse behavior (18).

67 Despite the fact that EF abrogation is a major determinant of problem behavior and
68 disability in neuropsychiatric disorders (19), the genetics underlying EF remains elusive with
69 no causative vector agents (e.g. genes) have yet been reported. Herein we show that *NTNG*
70 paralogs affecting human IQ also affect mouse learning and brain executive functioning.

71 RESULTS

72

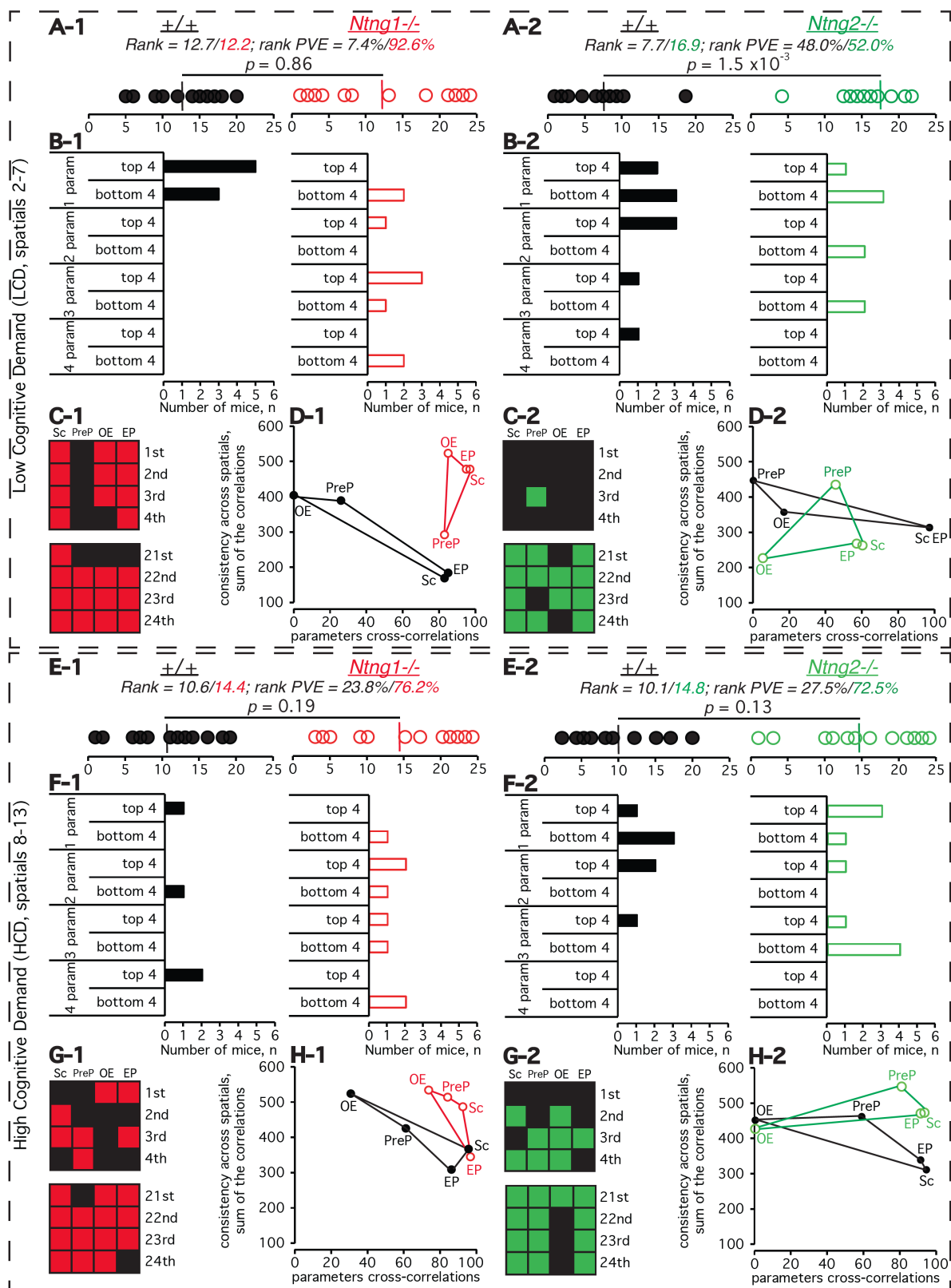
73 **Randomizing mouse genotypes to search for causal behavioral interactions.** We used a
74 novel non-parametric data analysis approach for two distinct behavioral paradigms: 5-choice
75 serial reaction time task (5-CSRTT, 20), and radial arm maze (RAM), measuring selective
76 attention and impulsivity (AI), and spatial working memory (WM), respectively, in *Ntng1*^{-/-}
77 and *Ntng2*^{-/-} mice. We calculated mouse genotype-independent ranking (as for a mixed
78 population), and the rank variance (as a proportion of variance explained, PVE) for each
79 behavioral parameter and for both paradigms. This approach allowed us to avoid common in
80 literature a genotype-attributed single parameter reporting bias (Supplementary Figures 1
81 (SF1) and 2 (SF2)), and permitted us to compare observed phenotypes between the both
82 paradigms for the genetically independent groups of mice, simultaneously searching for
83 potential interactions among them. We were able to follow the dynamics of behavioral
84 heterogeneity and to deduce a causal inference between the mouse phenotypic and genotypic
85 traits interaction affecting executive function (EF).

86

87 **Affected AI for both *Ntng* paralogs, and WM for the *Ntng2* gene, modulated by the**
88 **cognitive demand.** Analysis of the 5-CSRTT data (ST1-1) has revealed that *Ntng1*^{-/-}
89 population of mice is characterised by an extreme span of its rank distribution (PVE>90%)
90 occupying not only bottom 4 but also top 4 rank positions and outcompeting their wild type
91 littermates (Fig.1(A-D)-1). *Ntng1* ablation generates mice with both strong proficit and
92 deficit of AI, extending far beyond a single affected parameter estimate (Fig.1C,G), but with
93 the averaged rank per a genotype undistinguishable of that of their wild type littermates, and
94 more than 90% of variance attributable to the *Ntng1*^{-/-} genotype (Fig.1A-1). A higher
95 cognitive demand task phase (HCD) reduces the rank variance down to 76% but at the
96 expense of a lower rank (Fig.1E-1), similarly to *Ntng2*^{-/-} mice (Fig.1E-2). During the low
97 cognitive demand task phase (LCD), contrary to *Ntng1*^{-/-} mice, *Ntng2*^{-/-} subjects' rank is
98 twice lower comparing to their genetically unmodified siblings but the rank variances are the
99 same (Fig.1(A-D)-2), and this is the main difference in the AI phenotype between the *Ntng*
100 paralog knockouts, attributable to the magnitude of the demand.

101 Robustness of the WM deficit upon *Ntng2* deletion in mice is the most prominently
102 evidenced by the bottom 4 mouse ranks, 13/12 out of 16 are occupied by the knockout mice
103 (Fig.2(A-G)-2) and by low behavioral consistency across the sessions and parameters cross-
104 correlations (Fig.2H-2) during the HCD. At the same time, the absence of *Ntng1* in mice
105 affected only the LCD sessions performance (Fig.2(A-D)-1) but did not render them

106 behaviorally distinguishable from the wild type littermates during the HCD (Fig.2(E-H)-1).



107 Figure 1. 5-choice serial reaction time task (5-CSRTT) for *Ntn1*^{-/-} and *Ntn2*^{-/-} mice. See figure legend overleaf.

108

109 **Proficit and deficit in learning associated with the *Ntn*^{-/-} genotypes.** The intricate
 110 segregation of the *Ntn*^{-/-} gene paralogs-associated behavioral phenotypes within the distinct
 111 modules of EF (Fig.3) has prompted us to analyse the operant conditioning learning (Ln) by

112 **Figures 1,2. Attention and Impulsivity (AI) and working memory (WM) estimate and**
113 **the effect of cognitive demand produced by the analysis of rank and its variance for**
114 ***Ntng1*^{-/-} and *Ntng2*^{-/-} mice. A,E.** Mice ranks and rank PVE (proportion of variance
115 explained) based on four parameter rank measures (SF1,2) as detailed in ST1-1,2-1 (for
116 *Ntng1*^{-/-}) and ST1-2,2-2 (for *Ntng2*^{-/-}). The rank sorting was done in a genotype-independent
117 manner. Ranking for each out of four parameters was done independently of other
118 parameters with a final re-ranking of the ranks sum to generate the final rank (shown). In
119 case of an equal sum of the ranks, the mice were given identical ranks. PVE was calculated
120 as a square of within genotype rank variance divided on the sum of each genotype variances
121 squares multiplied on 100%. **B,F.** Mice rank distribution across one-to-four parameters as
122 top 4 and bottom 4 performers. **C,G.** Genotype-specific rank placing among the mice. **D,H.**
123 Behavioral consistency of mice across the sessions (*y* axis, sum of *r*² correlations of a single
124 session ranks *vs.* final ranks for each mouse across the sessions) and behavioral parameter
125 cross-correlations (*x* axis, the *r*² correlation of a parameter final ranking *vs.* final ranking for
126 all 4 parameters). The gene ablation-specific phenotype severity can be assessed visually by
127 matching each parameter-corresponding vertexes of the obtained quadruples. *p* value
128 represents a Wilcoxon rank sum test. See SM for further details.

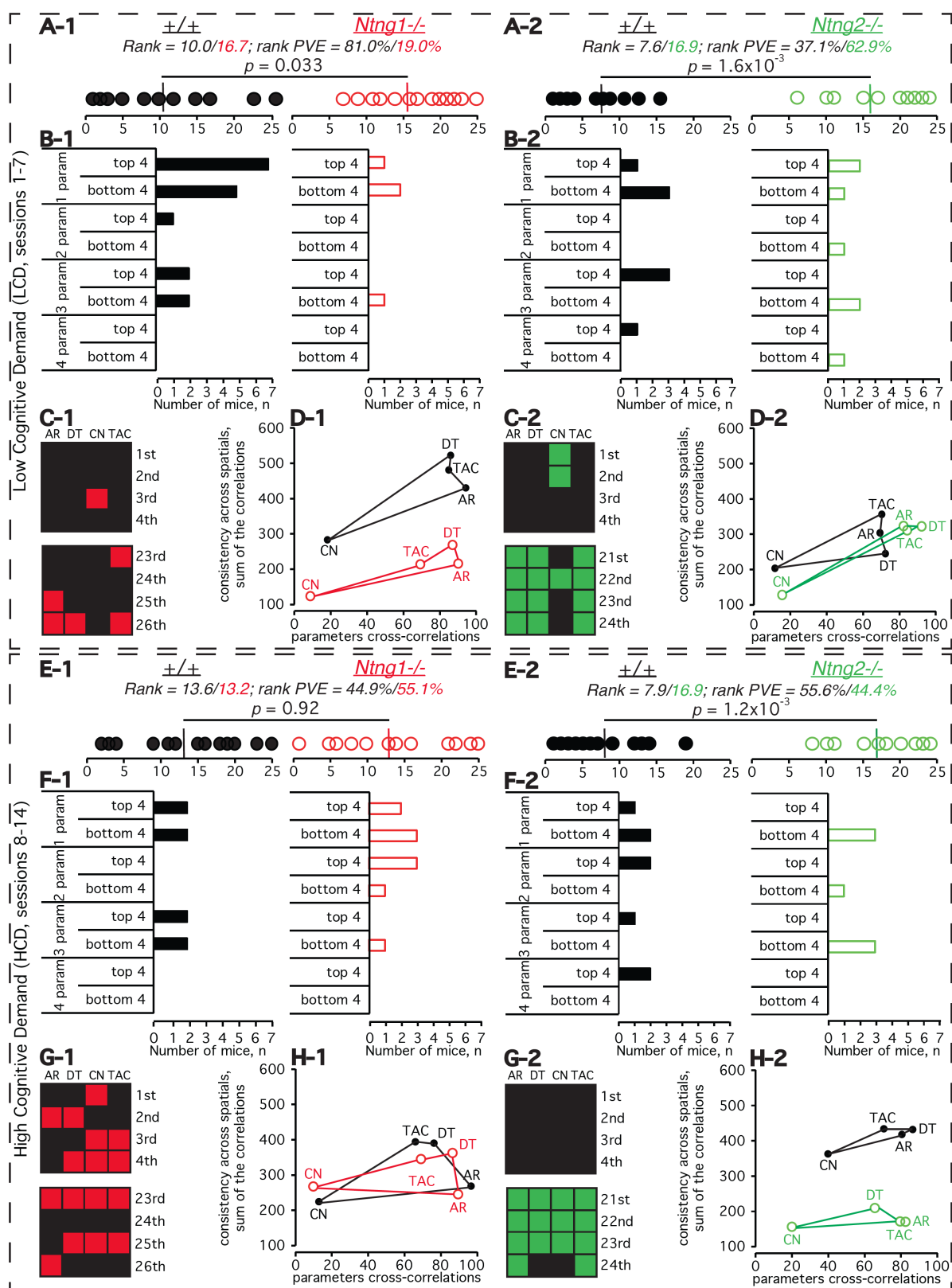
129

130 mice, assuming that AI and WM may there interact. And indeed, *Ntng1*^{-/-} mice outperform
131 their control group learning faster during the LCD (Fig.4(A,B)-1, LCD) but are unable to
132 sustainably cope with the growing cognitive demand (Fig.4(A,B)-1, HCD). At the same
133 time, *Ntng2*^{-/-} mice display a prominent deficit of Ln (Fig.4(A,B)-2, LCD), which is
134 becoming stronger with the growing demand to succeed (Fig.4(A,B)-2, HCD). In overall, the
135 pattern of Ln behavior caused by the genetic ablation of both *Ntngs* completely matches that
136 of WM testing on the RAM (Fig.2), summarised in Fig.3. The contribution of AI to the Ln
137 deficit is further demonstrated by the rank correlations of Ln *vs.* AI (from Fig.1) which is
138 stronger during the HCD for both genetically distinct mouse populations (Fig.4C-1,2).

139

140 **Complementary expression of *Ntng* paralogs in the brain and their interaction.** The
141 robust phenotype of the abrogated EF for both *Ntng* gene paralogs affecting either AI or
142 WM, or both, is supported by the predominant expression of both genes within the heavily
143 loaded with the information processing brain areas, complementary sequestering them within
144 bottom-up (for *Ntng1*) and top-down (for *Ntng2*) neuronal pathways (Fig.5A-C). The
145 presented hierarchy for the *Ntng* paralogs brain distribution is supported by two times lower
146 level of the *Ntng2* expression in *Ntng1*^{-/-} background after the life-long cognitive training in

147 senile mice (Fig.5D-2), with no effect on *Ntng1* expression when *Ntng2* is absent (Fig.5D-1).



148 Figure 2. Radial arm maze (RAM) for *Ntng1*^{-/-} and *Ntng2*^{-/-} mice. See figure legend overleaf.

149

150 **Robust genotype prediction based on the phenotype input, the rank.** To assess the causal
 151 inference of the genes perturbations on behavioral output we have calculated the probability
 152 clustering for each genotype based only on the ranking data input, in genotype-blind manner

153 (Fig.6A). The obtained pattern corroborates the causal relationship between the genotypes
154 and associated with them phenotypes of the affected EF (Fig.3) closely resembling the
155 experimental data (Fig.1.2).

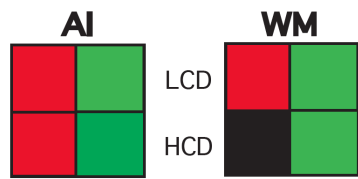


Figure 3. Summary of the EF behavioral phenotypes associated with either *Ntn1*^{-/-} or *Ntn2*^{-/-} gene paralogs ablation.

156

157 **Mouse behavioral phenotypic proximity assessment.** To calculate a phenotypic distance
158 between the genotypes comprising a single mixed population we used the obtained ranks and
159 plotted them against the related PVE for each behavioral parameter, generating two linear
160 plots (Fig.6B), each representing a single contributing genotype. This let us further to
161 calculate the phenotypic distance (using the classical Euclidean geometry) between the
162 genotypes as the shortest distance between two parallel lines. The obtained geometrical plots
163 are in a full agreement with the experimentally observed behaviors (Figs.1-3) but
164 additionally pinpoint the contribution of each individual parameter sometimes located outside
165 of the main cluster with others, e.g. PreP for the *Ntn1*^{-/-} (Fig.6B-1, AI-LCD), OE for the
166 *Ntn1*^{-/-} (Fig.6B-2, AI-HCD), and CN for the *Ntn2*^{-/-} (Fig.6B-2, WM-LCD). Using the Ln
167 rank and its PVE from Fig.4 as (x,y) coordinates we have assessed the phenotypic proximity
168 of the *Ntn1*^{-/-} and *Ntn2*^{-/-} mouse AI and WM phenotypes to the Ln deficit.

169

170 **Task learning (Ln) as an outcome of AI and MW interactions.** With the assumption that
171 shorter distance from the Ln coordinates to the genotype-specific linear plot generates higher
172 likelihood that the given genotype contributes to the Ln associated behavior, we were able to
173 build a relationship graph among the Ln, AI and WM interactions modulated by the
174 cognitive demand (Fig.7A). The dynamics of the *Ntn* gene paralogs hierarchy interaction is
175 presented on Fig.7B, calculated by the reciprocal plug-in of the rank and its PVE for one
176 gene paralog into the linear plot for the other one (ST7).

177

178 DISCUSSION

179

180 **Inferring causal relationship for the *Ntn* paralogs ablation caused perturbations with**
181 **the EF abrogation phenotypes.** The hierarchy of WM and selective attention interplay has
182 been always a point of fierce debate (21). In the present study we look at this interaction
183 through the prism of mouse operant conditioning learning ability, perturbed by either of

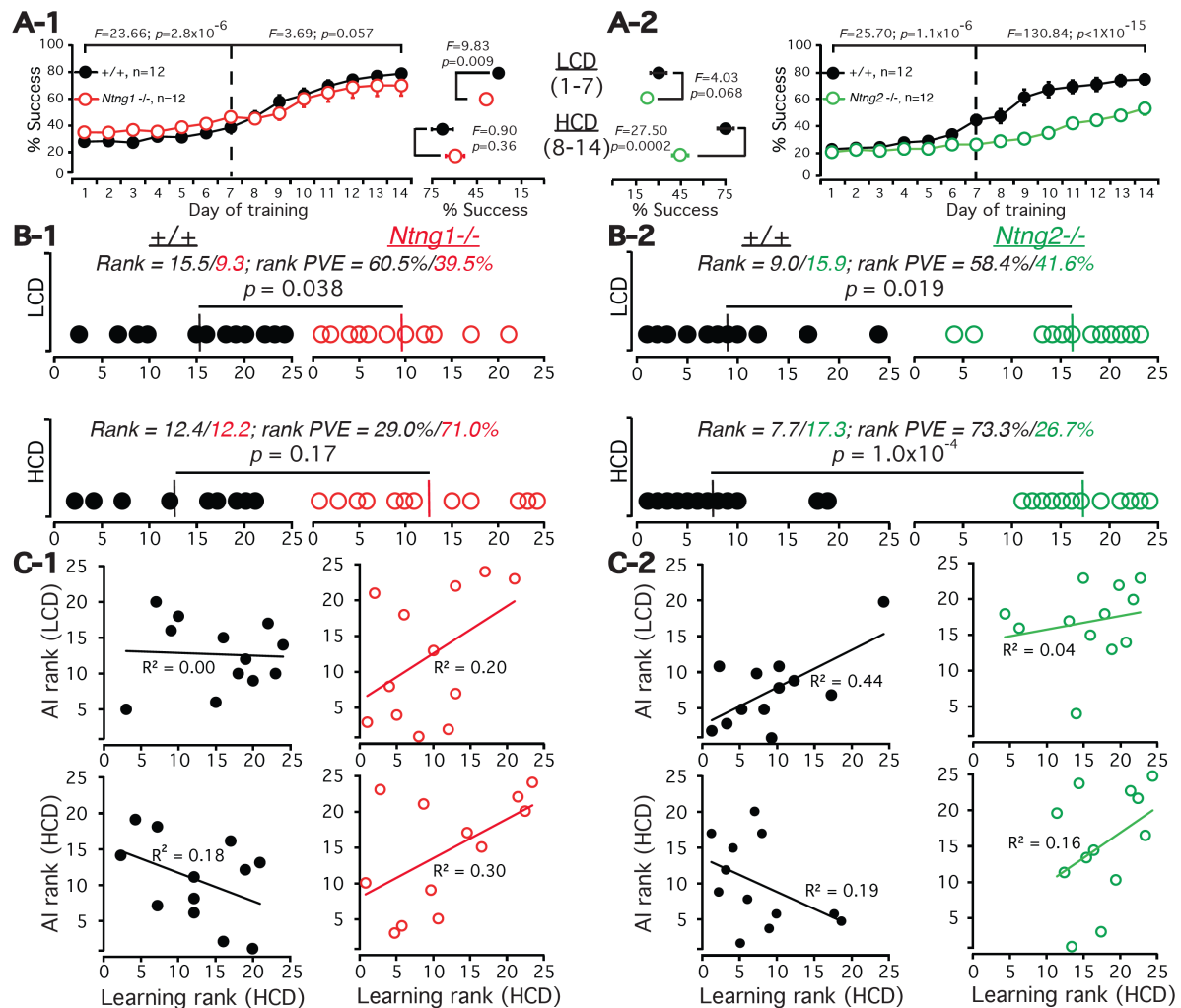


Figure 4. Operant conditioning (5-CSRTT) Learning (Ln) by *Ntn1*^{-/-} and *Ntn2*^{-/-} mice. A. Learning curves for the operant conditioning learning (reward collection) over the training period (spatial 1 of 5-CSRTT) with averaged performance behavior for the days (1-7) and (8-14), middle panel, defined as low cognitive demand (LCD) and high cognitive demand (HCD) sessions, respectively. One and two-way ANOVA was used for the statistics. B. Ranks and PVE comparisons over the LCD and HCD. The rank sorting was done in a genotype-independent manner, similar to Fig.1 and Fig.2, but using only one parameter, success (Sc), see ST4-1 and ST4-2. Rank statistics was by Wilcoxon rank sum test. C. Learning (Ln) vs. attention and impulsivity (AI) rank correlations (from Fig.1A-1,2).

184

185

186 *Ntn* gene paralogs ablation (Fig.4). Since it is known that averaging animal behavior across
 187 individual subjects (SF1-1,1-2) may smear out control variables (22), we used rank instead
 188 of classical data mean (Figs.1-3) approach and the rank variance (proportion of variance
 189 explained, PVE) per genotype, as a measure of difference (23:p.16), to assess the behavioral
 190 variability caused by the genetic variations interacting with the experimental demand. To
 191 proof causal inferences between the behavior of *Ntn*^{-/-} mice and the gene ablation, we used
 192 mouse rank as a randomized dependent variable of the mixed population noting that any
 193 other non-randomized variables would be only correlational (24). That is, we have presented
 194 the mouse behavioral rank distribution as a function of genotype, when one of the *Ntn*

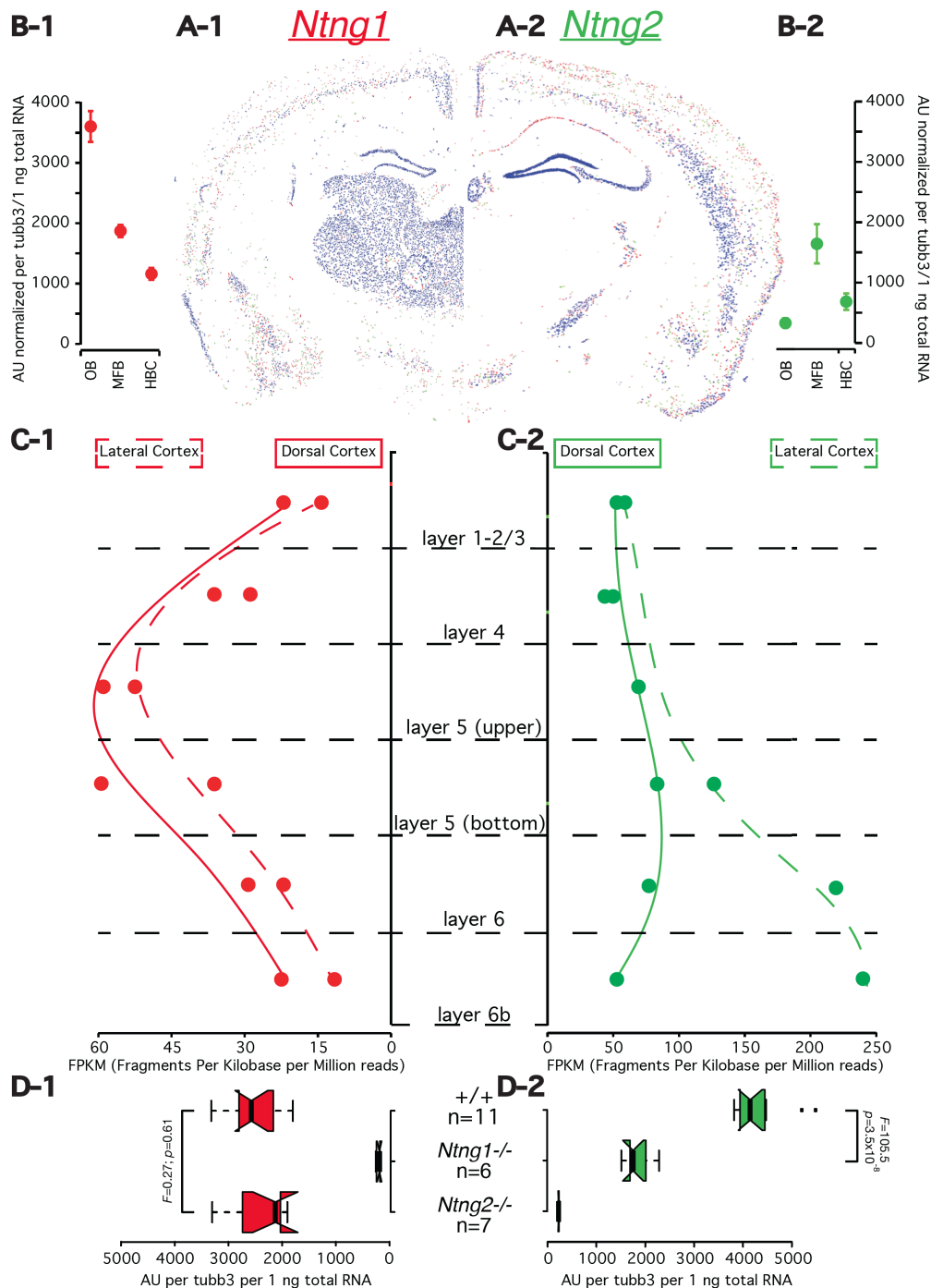


Figure 5. Complementary expression and transcription of *Ntng* paralogs in the mouse brain. (A) *In situ* hybridization of *Ntng1* (left) and *Ntng2* (right) in the mouse brain. From Allen Brain Atlas, accession numbers are RP_050607_01_H05 and RP_050810_04_D08, respectively. The expression colors are inverted. (B) qRT-PCR of total mRNA for *Ntng* paralogs in rough brain fractions of adult naïve male mice (7-8 months old): OB = olfactory bulb; MFB = mid- and front brain; HBC = hindbrain and cerebellum, n=6 mice (ST5-1). (C) Total level of *Ntng* mRNA expression calculated based on RNA-seq of the mouse brain cortical layers reconstructed for *Ntng* paralogs expression from GSE27243 generated by Belgard et al. (51). See Supplementary Methods (SM) for the details of data processing, ST5-2, ST5-2_Cuff and ST5-2_iReck (zipped) for the transcriptome assembly. (D) Effect of genetic background on *Ntng* paralogs expression level in MFB as detected by qRT-PCR (ST5-3). Senile (20-21 months old) life-long cognitively trained mice have been used (from Fig.1). One-way ANOVA was used for the statistics.

195

196

197

198

paralogs has been genetically ablated. At the same time, we have tried to elaborate on the statement that the structure of genotype–phenotype map is the matter and not the variance components of the population itself (25). The open question in such genotype-phenotype

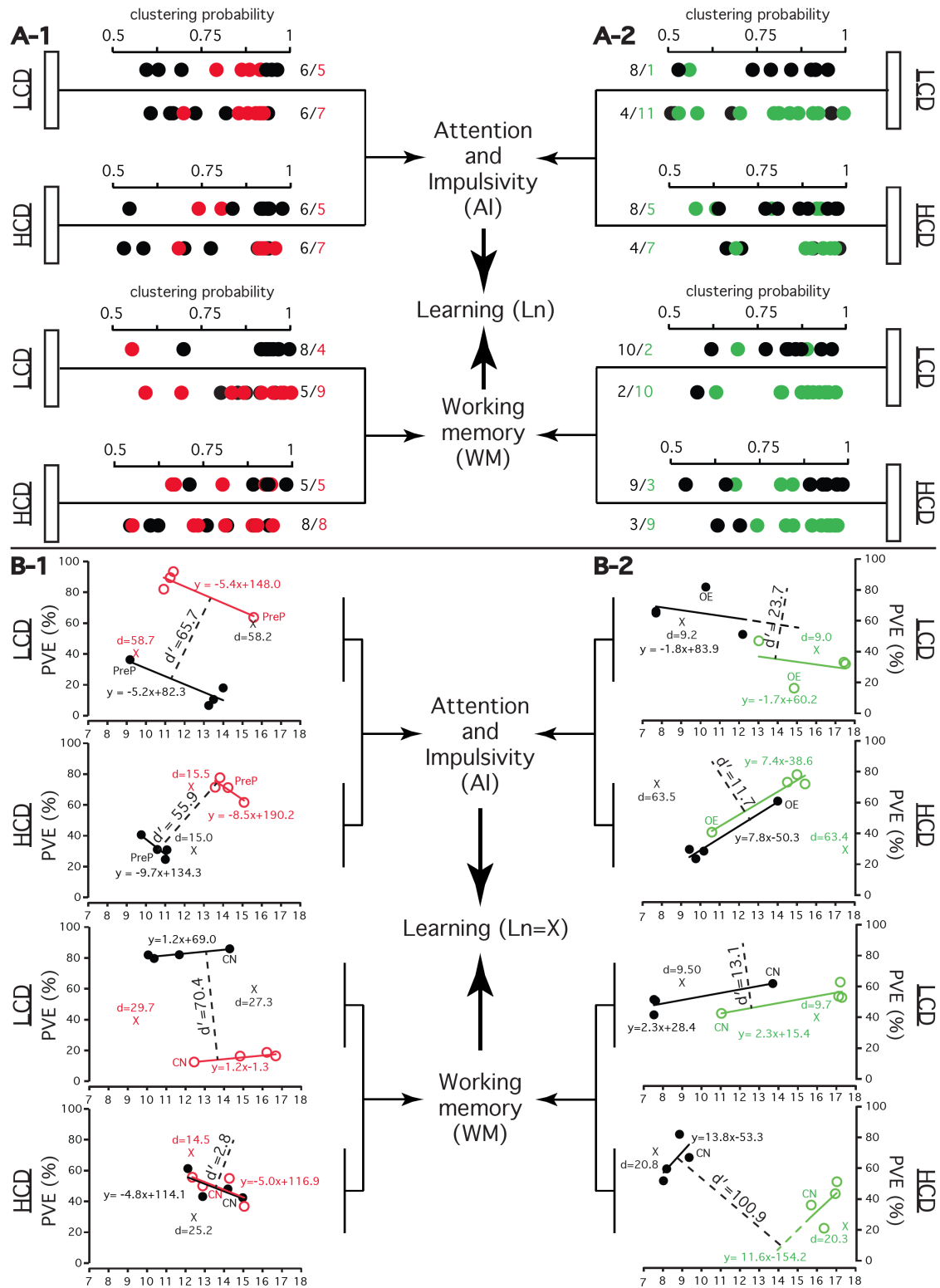


Figure 6. Behavioral phenotypic proximity assessment for the *Ntn1*^{-/-} and *Ntn2*^{-/-} genotypes and their wild type littermates by two approaches: genotype predictions by *C*-means fuzzy clustering (A), and by linear regression plot of genotype-specific rank PVE vs. rank (B). **A.** Casual genotype-phenotype relationship evidence. *C*-means fuzzy clustering (Euclidean *C*-means) was done in a genotype-blind manner as described in SM. See ST6-1 and ST6-2 for the exact values of clustering probabilities. **B.** Descriptive proximity of the operant conditioning learning explained by the AI and WM phenotypes for *Ntn1*^{-/-} paralog mice. Distance between the genotypes (d' , dashed line), presented geometrically by the linear equation, was calculated as $d' = |c_2 - c_1|$, where $ax + by + c = 0$ (Euclidean geometry). Distance from the learning coordinates (L_n) to the genotype-describing line was calculated as $d = |c - (y_{L_n} - ax_{L_n})|$. Rank (x coordinates) and PVE values (y coordinates) are from Fig. 1A,E (AI); Fig. 2A,E (WM); and Fig. 4B (L_n), ST7. Data for the *Ntn1*^{-/-}/wt population (RAM) are likely to incorporate 7.69% error since they were not normalised to the total number of animals as for the other populations ($n = 26$ vs. $n = 24$ mice).

200 interaction paradigm is to what degree a genetic variability is capacitive enough to explain
201 the phenotypic variance and the strength of such causal interaction. More specifically, how
202 far the behavioral (whole organism) variability (under the pressure of the growing cognitive
203 demand) represents the neuronal (cellular) variability caused by a gene knockout exerted
204 perturbations.

205

206 **Cognitive phenotypes of the *Ntng*^{-/-} mice.** None of the vertebrate brain specific
207 presynaptically expressed *Ntng1*^{-/-} nor *Ntng2*^{-/-} mice exhibit gross anatomical or
208 developmental abnormalities (26) rendering them unique models to study the brain cognitive
209 functions in the absence of any “house-keeping” functional distortions and avoiding gene-
210 manipulations-exerted non-causal confounders. Noteworthy the resemblance of *Ntng1*^{-/-} and
211 *Ntng2*^{-/-} mice behavioral phenotypes with the human schizophrenia subjects behavioral
212 etiology (characterised by the EF control pathologies), both genes have been reportedly
213 associated with (1,2). Two different populations of mice were used for two different
214 behavioral paradigms to avoid the phenomena of learning transfer between the behavioral
215 tests, and, at the same time, to check for the genotype induced phenotypic stability across the
216 different paradigms but sharing the principal underlying component of WM testing. And
217 indeed, slow operant conditioning learning (5-CSRTT) for *Ntng2*^{-/-} mice has been recorded
218 (Fig.4A,B-2) and is explainable by the dysfunction of procedural (working) memory robustly
219 affecting the RAM performance (Fig.2A-H-2).

220

221 **Behavior consistency assessment using rank.** We have also characterised the behavior of
222 mice as a heterogeneously randomized population through the assessment of rank
223 consistency across the sessions and relative to other parameters (Figs.1-2D,H). Parameters
224 cross-correlation coefficients (r^2 , x axis) indicate a probability value of how much the rank
225 of a mouse for a certain parameter contributes to the global (total) ranking comprised of all
226 four parameters. If a mouse fails to keep its performance consistent either over the multiple
227 sessions or a parameter, its rank is instantly occupied either by the same or by a different
228 genotype littermate, and such event would be dynamically reflected in the r^2 . But ranks
229 changes and their permutations may not necessary have any dramatic consequences in the
230 total rank calculations as soon the rank fluctuations are taking place within the same
231 genotype-specific variance boundaries. But they are more reflective of a behavior
232 inconsistency of an individual mouse reflected in the sum of the correlation variances per
233 spatial or session (y axis).

234

235 **WM deficit driven optimal strategy deprivation for the *Ntng2*^{-/-} mice.** The global spatial
 236 WM deficit for the *Ntng2*^{-/-} mice has been found robustly expressed across the three RAM
 237 parameters (Fig.2A-H-2) except for CN (arm choice number during the first 8 arm entries).
 238 This parameter represents a strategy development (during LCD) and its optimisation (during
 239 HCD) for the maximum reward collection efficiency, akin predictive type behavior of the
 240 likelihood of potential success. The fact that the *Ntng2*^{-/-} mice outperform their wt littermates
 241 in CN (but during the LCD only, Fig.2C-2) reflects the chosen strategy (or a complete lack
 242 of any) of a pure random choice of a baited arm to visit, corroborating the global WM deficit
 243 (inability for strategic thinking) for the knockouts (evident from the other parameters) but
 244 with an opposite valence.

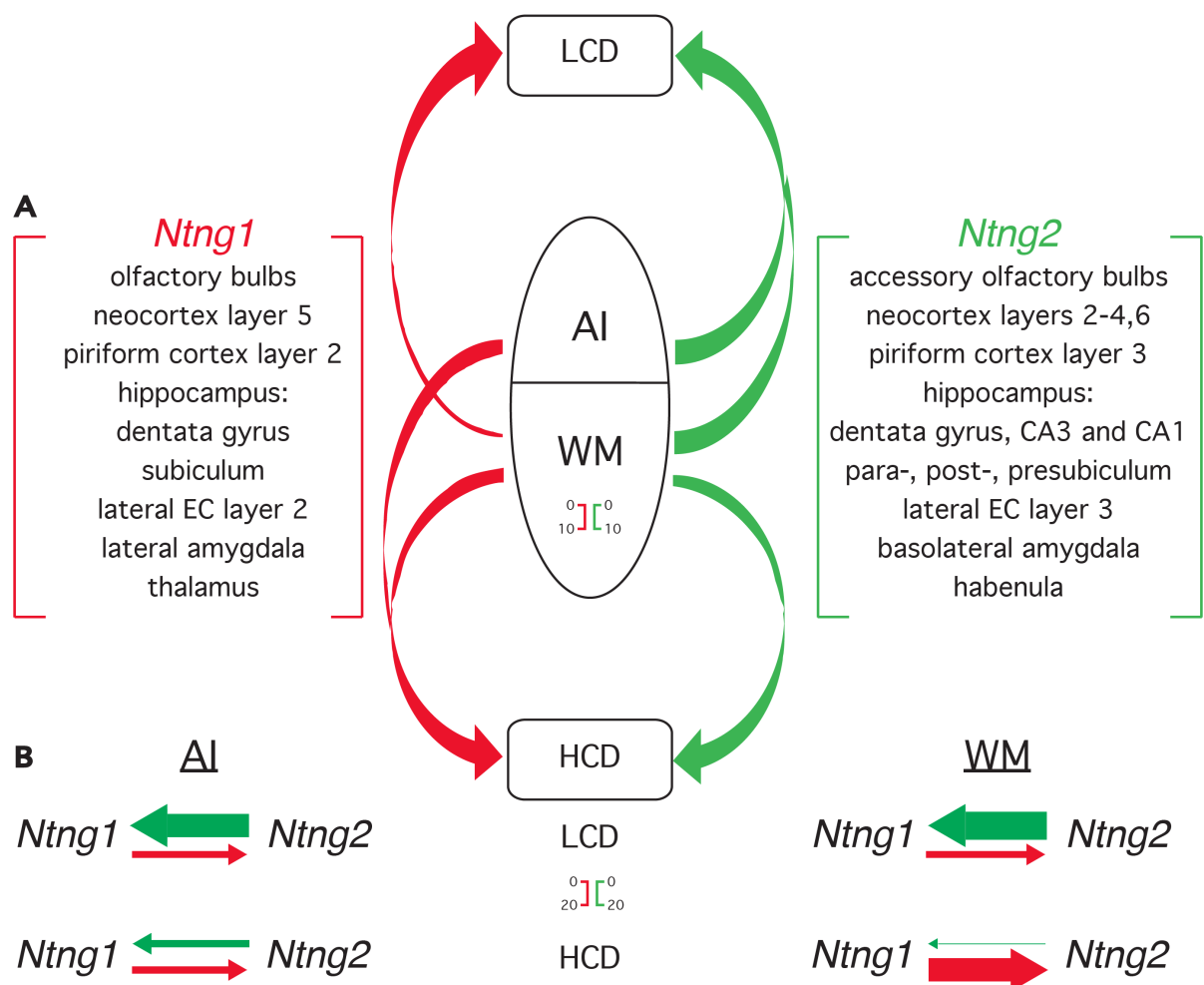


Figure 7. *Ntng* paralogs interaction as a molecular correlate of AI and WM modalities during learning. A. AI and WM interactions modulated by the cognitive demand during the operant conditioning earning (Ln), complementary contributed by the differentially expressed *Ntng* paralogs (see Fig.5 and (52)). B. Dynamicity of *Ntng* paralogs hierarchy interactions under LCD and HCD contributing to AI and WM. Each arrow base width (the scale bar is shown) is expressed in AU and corresponds to $(1/d*100)$ value from Fig.6B (for Ln=X), see ST7. Out of scale arrows (AI-*Ntng1*-LCD and AI-*Ntng2*-HCD) are not shown.

245

246

247 **Paralogs brain expression supporting the behavioral phenotypes.** The phenotypic

248 complementarities among the *Ntng1*^{-/-} and *Ntng2*^{-/-} mice, associated either with the abrogated
249 AI or WM, or both (Fig.3), are supported by the complementary brain expression pattern of
250 these gene paralogs (Fig.5A). If *Ntng1* is expressed mostly in the primary somatosensory
251 gating areas (e.g. OB, thalamus and hypothalamus nuclei, midbrain and medulla, Fig.5A,B-
252 1), *Ntng2* dominates within the cortex (with the skewed expression saturation towards the
253 lateral cortex), hippocampus (HPC), amygdala and claustrum, endopiriform and reticular
254 nuclei, Fig5A-2), pointing the gene role of parsing top-down signals. If the sensory
255 perception, as an entry point into the attentional state, is determined by the strength of the
256 subcortical thalamus-PFC (pre-frontal cortex) pathways (27), the reciprocal interactions
257 between mPFC and HPC are pivotal for the WM functioning (28,29), with the HPC known
258 to encode perceptual representations into memories through the correct attentional states
259 (30). Complementing this, thalamocortical projections are vital for mediating sensation,
260 perception, and consciousness (31-33). It is assumed that WM, despite its distributed nature
261 (34), consists of an executive component spread over the frontal lobes and sensory cortices
262 and interacted by the attention (7,35).

263

264 **Brain lamina-specific enrichment and EF control contribution by the *Ntng* paralogs.**

265 The emergence of a six-layered neocortex is a known hallmark of the mammalian brain
266 specialization devoted to the EF control (36,37). Both *Ntng* gene paralogs are extensively
267 expressed and mutually sequestered among the separate layers of the cortex (Fig.5C). *Ntng1*
268 is predominantly located in layers 4/5 (Fig.5C-1), probably supporting the arrival of the
269 bottom-up signals (38), while *Ntng2* is located in the superficial layers 2/3 and deeper layers
270 5/6 (Fig.5C-2), reported as a source of top-down inputs in attention and WM demanding
271 tasks (39). Besides that, *Ntng2* has been also marked as a gene classifier for the granule
272 neurons enriched in the cortex layer 6 (40). In overall, the complementary patterning of the
273 *Ntng* gene paralogs expression supports the laminar-specific distribution of the attention-
274 directed modalities.

275

276 **Evidence for the cognitive control taking over the perceptual load.** Analysing AI and
277 WM interaction during the task learning (Fig.7A), we have revealed that HCD recruits more
278 *Ntng1* (bottom-up) expressing circuitry comparing to LCD, both by WM and AI, reciprocally
279 replacing the preceding *Ntng2* (top-down) contribution. This potentially points to an
280 augmented peripheral sensory control by upregulating the bottom-up information stream.
281 How to explain such intricacy? Attention exploits a conserved circuitry motif predating the
282 neocortex emergence (41) and WM probably exapts the motor control of forward action

283 modeling also elaborated since ancient times (42). The archaic origin of both modalities
284 limits the fundamental brain resource and constrains information processing, forcing trade-
285 offs among the objects of targeted attention through the top-down control and, possibly,
286 causing a competition between the sensory inputs (43,44) by driving attention at
287 representations in sensory areas where the latter gains entry into WM (7). A model has been
288 proposed that selective attention control is directly linked to the executive control part of the
289 WM system (45) corroborating the statement that attention and WM should no longer be
290 regarded as two separate concepts, see (46) for references. The top-down control of primary
291 sensory processing by higher cortical areas (through the recurrent inputs) has an essential
292 role in sensory perception, as we have just demonstrated. The pervasive penetration of the
293 cognitive control, supported by *Ntn2*, affects the sensory inputs, provided by the *Ntn1*
294 expression.

295

296 **An IQ for mice.** The EF control variance attributes to the cognitive performance variance
297 and does not exist independently of general intelligence (47) as a critical determinant of
298 human cognition (48). It is no wonder then that, in our hands, the genes affecting WM and
299 attention in mice are the same ones affecting IQ in humans (1) and also associated with a
300 variety of devastating neurological disorders (2) representing a strong case of antagonistic
301 functional pleiotropy. The open challenge is to find out to what degree, using *Ntn* gene
302 paralogs as benchmarks, we would be able to conclusively draw on either domain specific or
303 domain general cognitive abilities of mice, or any other non-human animal subjects
304 behavioral intelligence.

305

306 Conclusively, *Ntn1* participates in bottom-up, and *Ntn2* in top-down brain
307 information flows support, representing an integrative complementary agreement between
308 perception and cognition as two interacting functions of the brain.

309

310 CONCLUSION

311

312 The view of Brain (and Mind) as a modular (domain) system is appealing to evolutionary
313 thinking (49) but is strongly biased towards “the prominence of neural reductionism” (22)
314 dominating the modern neuroscience. There is no strict definition of what a cognitive domain
315 is but it can be viewed as a product of interaction between the top-down and bottom-up
316 underlying neuronal circuits forming bidirectional feedback loops for the executively
317 decisive and sensory information flows controlling its own self. Genes selectively expressed

318 within such circuits via a non-overlapping pattern represent a tantalizing target to study the
319 cognitive domain make-up and its evolution. An ancient *Ntng* gene duplication (>500 million
320 years ago, preceding the Cambrian explosion) and subsequent co-evolution within the
321 vertebrate genomes made *Ntng* gene paralogs to segregate within the top-down and bottom-
322 up evolving information paths, presumably via subfunctionalisation, under the growing
323 ecological demand (first land/water fish met) but different epistatic environment, both gene
324 paralogs are embedded into. Perception and cognition interplay had eventually culminated
325 in a reflectively subjective representation of the external world, also called consciousness,
326 and explicitly controlled by the EF. Unrevealing molecular correlates of the domain-specific
327 cognitive abilities would help us better understand behavior, e.g. to clearly dissect it on
328 actions (as self-generated thoughts) and responses (cue-induced actions), as a decomposable
329 conjunction supporting the robust functioning of the Brain holistic state.

330

331 MATERIALS AND METHODS

332

333 **Animals and behavioral set-ups.** Animal rearing and handling experimental procedures
334 were performed in accordance with the guidelines of RIKEN Institutional Animal Care and
335 Experimentation Committee. The original behavioral datasets have been partially published
336 by us in (18). All raw data are provided in [ST1-ST4](#) and [SF1,2](#). Knockout animals generation
337 and the behavioral set-ups are described in (18).

338

339 **Data analysis.** All raw data including their ranks and PVE calculations with all formulas and
340 graphs are presented in [ST1-ST4](#). The dynamics of the rank change for a specific parameter
341 over the course of study and its congruence with other parameters is depicted on [Figs.1-
342 2D,H](#). No robustness calculations of the rank distribution pattern resistance to a sequential
343 removal of a single behavioral subject were done; neither estimate for the minimal number of
344 the top/bottom ranks representing the obtained pattern, it was empirically decided to be equal
345 to top and bottom four ([Figs.1-2](#)).

346

347 **Definition of LCD and HCD.** During the 5-CSRTT the cognitive demand was incremented
348 by a shorter cue duration and longer inter-trial intervals, as specified in (18). As for the
349 RAM, the second week of testing (sessions 8-14) was done with half-closed/half-opened
350 doors under the gradually building cognitive demand, internally driven by the behavior
351 optimisation strategy for the maximum likelihood of reward collection, top-down executive-
352 attentional pressure to optimise the behavioral performance outcome, contextually similar to

353 the operant conditioning learning (Ln) of spatial 1 of the 5-CSRTT (Fig.4).

354

355 **Real-time qPCR (qRT-PCR).** Primers specifically targeting beginning of each *Ntng* gene
356 paralogs full-length transcripts were designed using Primer3Plus:
357 <http://www.bioinformatics.nl/cgi-bin/primer3plus/primer3plus.cgi>. Frozen brains RNA was
358 isolated from the MFB using RNeasy Plus Minikit (Qiagen) and the cDNA was synthesised
359 by the QuantiTect[®] Reverse Transcription kit (Qiagen) using a mix of the random hexamers
360 and oligodT primers. cDNA synthesised from 1 ng of total RNA was used per a single qRT-
361 PCR reaction. The lack of genomic DNA and the absence of external contamination were
362 confirmed by the RT-minus reactions. Neuronal-specific *tubb3* transcript (β -tubulinIII) was
363 used as an internal normaliser during the qRT-PCR co-amplifications. The C_t values were
364 collected at the threshold value of 0.4 and the arbitrary units (AU) were calculated as:

$$365 \quad 2^{-(C_t(\text{amplicon}) - C_t(\text{normalizer}))} * 10,000$$

366

367 **RNA-seq cortical layers *Ntng* transcriptome reconstruction.** See SM for the details.

368

369 **Fuzzy C-Means Clustering.** Represents a type of a sequential competitive learning
370 algorithm exhibiting the stochastic approximation problem (50). Was used for the genotype
371 predictions based on the behavioral ranks input under the genotype-blind input conditions.
372 The details are described in the SM.

373

374 **Statistics.** Correlation coefficients (r^2) were obtained with Excel. One and two-way
375 ANOVA was calculated using StatPlus (AnalystSoft Inc.). Wilcoxon rank sum test was done
376 by Matlab (v.7.9.0 2009b) by the function *ranksum*.

377

378 SUPPLEMENTARY MATERIALS (SM)

379 Contain Supplementary Figures (SF1-2), Tables (ST1-7), Methods and References. ST1-ST5
380 are provided as Excel files.

381

382 ACKNOWLEDGEMENTS

383 This work was in part supported by the “Funding Program for World-Leading Innovative
384 R&D on Science and Technology (FIRST Program)” initiated by the Council for Science
385 and Technology Policy (CSTP), and KAKENHI 15H04290 from the Japan Society for the
386 Promotion of Science (JSPS).

387

388 COMPETING INTERESTS

389 Authors would like to express a lack of any competing interests associated with the work.

390 REFERENCES

391

- 392 1. Prosselkov P, Hashimoto R, Polygalov D, Ohi K, Zhang Q, McHugh JT, Takeda M, and
393 Itohara, S. (2016) Cognitive endophenotypes of modern and extinct hominins associated
394 with *NTNG* gene paralogs. *Biomedical Genetics and Genomics*, **1**(1): 5–13.
395 <http://doi.org/10.15761/BGG.1000103>
- 396 2. Prosselkov P, Polygalov D, Zhang Q, McHugh JT and Itohara S. (2016) Cognitive domains
397 function complementation by *NTNG* gene paralogs. *Biomedical Genetics and Genomics*,
398 **1**(1): 24–33. <http://doi.org/10.15761/BGG.1000105>
- 399 3. Mar AC, Horner AE, Nilsson SRO, Alsio J, Kent BA, Kim CH, Holmes A, Saksida LM,
400 Bussey TJ. (2013) The touchscreen operant platform for assessing executive function in
401 rats and mice. *Nature Protocols*, **8**(10): 1985–2005. <http://doi.org/10.1038/nprot.2013.123>
- 402 4. Mandelman SD and Grigorenko EI (2011) "Intelligence". In *The Cambridge Handbook of*
403 *Intelligence*. Edited by Sternberg RJ and Kaufmann SB. Cambridge University Press.
404 ISBN: 052173911X.
- 405 5. Matzel LD and Kolata S. (2010) Selective attention, working memory, and animal
406 intelligence. *Neuroscience and Biobehavioral Reviews*, **34**(1): 23–30.
407 <http://doi.org/10.1016/j.neubiorev.2009.07.002>
- 408 6. Baddeley A. (1992) Working Memory. *Science*, **255**(5044): 556–559.
409 <http://doi.org/10.1126/science.1736359>
- 410 7. Carruthers P. (2013) Evolution of working memory. *Proceedings of the National Academy*
411 *of Sciences of the United States of America*, **110**(S2): 10371–10378.
412 <http://doi.org/10.1073/pnas.1301195110>
- 413 8. Trubutschek D, Marti S, Ojeda A, King J-R, Mi Y, Tsodyks M and Dehaene S. (2016) A
414 theory of working memory without consciousness or sustained activity. *bioRxiv*.
415 <http://doi.org/https://doi.org/10.1101/093815>
- 416 9. Soto D and Silvanto J. (2014) Reappraising the relationship between working memory and
417 conscious awareness. *Trends in Cognitive Sciences*, **18**(10): 520–525.
418 <http://doi.org/http://dx.doi.org/10.1016/j.tics.2014.06.005>
- 419 10. Leong YC, Radulescu A, Daniel R, DeWoskin V and Niv Y. (2017) Dynamic Interaction
420 between Reinforcement Learning and Attention in Multidimensional Environments.
421 *Neuron*, **93**(2): 451–463. <http://doi.org/10.1016/j.neuron.2016.12.040>

- 422 11. Cahen A and Tacca MC. (2013) Linking perception and cognition. *Frontiers in*
423 *Psychology*, **4**: e144. <http://doi.org/10.3389/fpsyg.2013.00144>
- 424 12. Potter MC. (2012) Conceptual Short Term Memory in Perception and Thought. *Frontiers*
425 *in Psychology*, **3**: e113. <http://doi.org/10.3389/fpsyg.2012.00113>
- 426 13. Brown H, Friston K and Bestmann S. (2011) Active Inference, Attention, and Motor
427 Preparation. *Frontiers in Psychology*, **2**: e218. <http://doi.org/10.3389/fpsyg.2011.00218>
- 428 14. Mroczko-Wąsowicz A. (2016) Editorial: Perception-Cognition Interface and Cross-Modal
429 Experiences: Insights into Unified Consciousness. *Frontiers in Psychology*, **7**: e1593.
430 <http://doi.org/10.3389/fpsyg.2016.01593>
- 431 15. Clark A. (2013) Whatever next? Predictive brains, situated agents, and the future of
432 cognitive science. *Behavioral and Brain Sciences*, **36**(3): 181–204.
433 <http://doi.org/10.1017/s0140525x12000477>
- 434 16. Rosenberg MD, Finn ES, Scheinost D, Constable RT and Chun MM. (2017)
435 Characterizing Attention with Predictive Network Models. *Trends in Cognitive Sciences*,
436 **21**(4): 290–302. <http://doi.org/10.1016/j.tics.2017.01.011>
- 437 17. Firestone C and Scholl CF. (2015) Cognition does not affect perception: Evaluating the
438 evidence for “top-down” effects. *Behavioral and Brain Sciences*, **39**: e229.
439 <http://doi.org/https://doi.org/10.1017/S0140525X15000965>
- 440 18. Zhang Q, Goto H, Akiyoshi-Nishimura S, Prosselkov P, Sano C, Matsukawa H, Yaguchi
441 K, Nakashiba T and Itohara S. (2016) Diversification of behavior and postsynaptic
442 properties by netrin-G presynaptic adhesion family proteins. *Molecular Brain*, **9**(1): e6.
443 <http://doi.org/10.1186/s13041-016-0187-5>
- 444 19. Royall DR, Lauterbach EC, Cummings JL, Reeve A, Rummans TA, Kaufer DI, LaFrance
445 CW, Coffey CE. (2002) Executive Control Function: A Review of Its Promise and
446 Challenges for Clinical Research. *The Journal of Neuropsychiatry and Clinical*
447 *Neurosciences*, **14**(4): 377–405. <http://doi.org/10.1176/jnp.14.4.377>
- 448 20. Bari A, Dalley JW and Robbins TW (2008) The application of the 5-choice serial reaction
449 time task for the assessment of visual attentional processes and impulse control in rats.
450 *Nature Protocols*, **3**(5), 759–767. <http://doi.org/10.1038/nprot.2008.41>
- 451 21. Abrahamse E, Majerus S, Fias W and Dijk J-P. (2015) Editorial: Turning the Mind’s Eye
452 Inward: The Interplay Between Selective Attention and Working Memory. *Frontiers in*
453 *Human Neuroscience*, **9**: (e616). <http://doi.org/10.3389/fnhum.2015.00616>
- 454 22. Gomez-Marin A and Mainen ZF. (2016) Expanding perspectives on cognition in humans,
455 animals, and machines. *Current Opinion in Neurobiology*, **37**: 85–91.
456 <http://doi.org/10.1016/j.conb.2016.01.011>

- 457 23. Laudański LM. (2013) *Between Certainty and Uncertainty: Statistics and Probability in*
458 *Five Units with Notes on Historical Origins and Illustrative Numerical Examples*
459 (Intelligent Systems Reference Library) Springer. ISBN-13: 978-3642256967.
- 460 24. Jazayeri M and Afraz A (2017) Navigating the Neural Space in Search of the Neural Code.
461 *Neuron*, **93**(5), 1003–1014. <http://doi.org/10.1016/j.neuron.2017.02.019>
- 462 25. Paixão T and Barton NH. (2016) The effect of gene interactions on the long-term response
463 to selection. *Proceedings of the National Academy of Sciences*, **113**(16): 4422–4427.
464 <http://doi.org/10.1073/pnas.1518830113>
- 465 26. Nishimura-Akiyoshi S, Niimi K, Nakashiba T and Itohara S. (2007) Axonal netrin-Gs
466 transneuronally determine lamina-specific subdendritic segments. *Proceedings of the*
467 *National Academy of Sciences of the United States of America*, **104**(37): 14801–14806.
468 <http://doi.org/10.1073/pnas.0706919104>
- 469 27. Wimmer RD, Schmitt LI, Davidson TJ, Nakajima M, Deisseroth K, Halassa MM. (2015)
470 Thalamic control of sensory selection in divided attention. *Nature*, **526**(7575): 705–709.
471 <http://doi.org/10.1038/nature15398>
- 472 28. Jin J and Maren S. (2015) Prefrontal-Hippocampal Interactions in Memory and Emotion.
473 *Frontiers in Systems Neuroscience*, **9**: e170. <http://doi.org/10.3389/fnsys.2015.00170>
- 474 29. Spellman T, Rigotti M, Ahmari SE, Fusi S, Gogos JA, Gordon JA. (2015) Hippocampal–
475 prefrontal input supports spatial encoding in working memory. *Nature*, **522**(7556): 309–
476 314. <http://doi.org/10.1038/nature14445>
- 477 30. Aly M and Turk-Browne NB (2016) Attention promotes episodic encoding by stabilizing
478 hippocampal representations. *Proceedings of the National Academy of Sciences of the*
479 *United States of America*, **113**(4): E420–429. <http://doi.org/10.1073/pnas.1518931113>
- 480 31. Riga D, Matos MR, Glas A, Smit AB, Spijker S and Oever MCV. (2014) Optogenetic
481 dissection of medial prefrontal cortex circuitry. *Frontiers in Systems Neuroscience*, **8**:
482 E230. <http://doi.org/10.3389/fnsys.2014.00230>
- 483 32. John ER. (2002) The neurophysics of consciousness. *Brain Research Reviews*, **39**(1): 1–
484 28. [http://dx.doi.org/10.1016/S0165-0173\(02\)00142-X](http://dx.doi.org/10.1016/S0165-0173(02)00142-X)
- 485 33. Alitto HJ and Usrey WM. (2003) Corticothalamic feedback and sensory processing.
486 *Current Opinion in Neurobiol.*, **13**(4): 440–445. [http://10.1016/S0959-4388\(03\)00096-5](http://10.1016/S0959-4388(03)00096-5)
- 487 34. Christophel TB, Klink PC, Spitzer B, Roelfsema PR and Haynes J-D. (2017) The
488 Distributed Nature of Working Memory. *Trends in Cognitive Sciences*, **21**(2): 111–124.
489 <http://doi.org/10.1016/j.tics.2016.12.007>
- 490 35. Postle BR. (2006) Working memory as an emergent property of the mind and brain.
491 *Neuroscience*, **139**(1): 23–38. <http://doi.org/10.1016/j.neuroscience.2005.06.005>

- 492 36. Smaers JB, Gómez-Robles A, Parks AN and Sherwood CC. (2017) Exceptional
493 Evolutionary Expansion of Prefrontal Cortex in Great Apes and Humans. *Current*
494 *Biology*, **27**(5): 714-720. <http://doi.org/10.1016/j.cub.2017.01.020>
- 495 37. Hardung S, Epple R, Jäckel Z, Eriksson D, Uran C, Senn V, Gibor L, Yiezhari O, Diester
496 I. (2017) A Functional Gradient in the Rodent Prefrontal Cortex Supports Behavioral
497 Inhibition. *Current Biology*, **27**(4): 549–555. <http://doi.org/10.1016/j.cub.2016.12.052>
- 498 38. Nandy AS, Nassi JJ and Reynolds JH. (2017) Laminar Organization of Attentional
499 Modulation in Macaque Visual Area V4. *Neuron*, **93**(1): 235–246.
500 <http://doi.org/10.1016/j.neuron.2016.11.029>
- 501 39. Kerkoerle T, Self MW and Roelfsema PR. (2017) Layer-specificity in the effects of
502 attention and working memory on activity in primary visual cortex. *Nature*
503 *Communications*, **8**: e13804. <http://doi.org/10.1038/ncomms13804>
- 504 40. Lake BB, Ai R, Kaeser GE, Salathia NS, Yung YC, Liu R, Wildberg A, Gao D, Fung H-L,
505 Chen S, Vijayaraghavan R, Wong J, Chen A, Sheng X, Kaper F, Shen R, Ronaghi M, Fan
506 J-B, Wang W, Chun J, Zhang, K. (2016) Neuronal subtypes and diversity revealed by
507 single-nucleus RNA sequencing of the human brain. *Science*, **352**(6293): 1586–1590.
508 <http://doi.org/10.1126/science.aaf1204>
- 509 41. Krauzlis RJ, Bollimunta A, Arcizet F, Wang L. (2014) Attention as an effect not a cause.
510 *Trend Cog Sci*, **18**(9): 457–464. <http://doi.org/http://dx.doi.org/10.1016/j.tics.2014.05.008>
- 511 42. Jeannerod M. (2006) *Motor Cognition*. Oxford University Press. ISBN: 0198569653
- 512 43. Koch C and Tsuchiya N. (2007) Attention and consciousness: two distinct brain processes.
513 *Trends in Cognitive Sciences*, **11**(1): 16–22. <http://doi.org/10.1016/j.tics.2006.10.012>
- 514 44. Boxtel JJA, Tsuchiya N and Koch C. (2010) Consciousness and attention: on sufficiency
515 and necessity. *Frontiers in Psychology*, **1**: e217. <http://doi.org/10.3389/fpsyg.2010.00217>
- 516 45. Vandierendonck A. (2014) Symbiosis of executive and selective attention in working
517 memory. *Frontiers in Hum Neurosci*, **8**: E588. <http://doi.org/10.3389/fnhum.2014.00588>
- 518 46. Quak M, London RE and Talsma D. (2015) A multisensory perspective of working
519 memory. *Frontiers in Hum Neurosci*, **9**: E197. <http://doi.org/10.3389/fnhum.2015.00197>
- 520 47. Royall DR and Palmer RF. (2014) “Executive functions” cannot be distinguished from
521 general intelligence: two variations on a single theme within a symphony of latent
522 variance. *Frontiers in Behav Neurosci*, **8**: E369. <http://doi.org/10.3389/fnbeh.2014.00369>
- 523 48. Lucenet J and Blaye A. (2014) Age-related changes in the temporal dynamics of executive
524 control: a study in 5- and 6-year-old children. *Frontiers in Psychology*, **5**: E831.
525 <http://doi.org/10.3389/fpsyg.2014.00831>

- 526 49. Burkart JM, Schubiger MN and Schaik CP. (2016) The evolution of general intelligence.
527 *Behavioral and Brain Sci*, **Jul 28**: 1–65. <http://doi.org/10.1017/S0140525X16000959>
- 528 50. Pal NR, Bezdek JC, and Hathaway RJ. (1996) Sequential Competitive Learning and the
529 Fuzzy *c*-Means Clustering Algorithms. *Neural Networks*, **9**(5): 787–796.
- 530 51. Belgard TG, Marques AC, Oliver PL, Abaan HO, Sirey TM, Hoerder-Suabedissen A,
531 García-Moreno F, Molnár Z, Margulies EH, Ponting CP. (2011) A Transcriptomic Atlas
532 of Mouse Neocortical Layers. *Neuron*, **71**(4): 605–616.
533 <http://doi.org/10.1016/j.neuron.2011.06.039>
- 534 52. Yaguchi K, Nishimura-Akiyoshi S, Kuroki S, Onodera T, Itohara S. (2014) Identification
535 of transcriptional regulatory elements for *Ntng1* and *Ntng2* genes in mice. *Molecular*
536 *Brain*, **7**(1): 19. <http://doi.org/10.1186/1756-6606-7-19>